Earthquakes and Structures, *Vol. 16, No. 3 (2019) 279-293*
DOI: https://doi.org/10.12989/eas.2019.16.3.279

Improvement of the cyclic response of RC columns with inadequate lap splices-Experimental and analytical investigation

George I. Kalogeropoulos[a] and Alexander-Dimitrios G. Tsonos*

Department of Civil Engineering, Aristotle University of Thessaloniki, GR-54-124 Thessaloniki, Greece

(Received January 8, 2019, Revised January 25, 2019, Accepted January 26, 2019)

Abstract. The overall seismic performance of existing pre 1960-70s reinforced concrete (RC) structures is significantly affected by the inadequate length of columns' lap-spliced reinforcement. Due to this crucial structural deficiency, the cyclic response is dominated by premature bond - slip failure, strength and stiffness degradation, poor energy dissipation capacity and low ductility. Recent earthquakes worldwide highlighted the importance of improving the load transfer mechanism between lap-spliced bars, while it was clearly demonstrated that the failure of lap splices may result in a devastating effect on structural integrity. Extensive experimental and analytical research was carried out herein, to evaluate the effectiveness and reliability of strengthening techniques applied to RC columns with lap-spliced reinforcement and also accurately predict the columns' response during an earthquake. Ten large scale cantilever column subassemblages, representative of columns found in existing pre 1970s RC structures, were constructed and strengthened by steel or RC jacketing. The enhanced specimens were imposed to earthquake-type loading and their lateral response was evaluated with respect to the hysteresis of two original and two control subassemblages. The main variables examined were the lap splice length, the steel jacket width and the amount of additional confinement offered by the jackets. Moreover, an analytical formulation proposed by Tsonos (2007a, 2019) was modified appropriately and applied to the lap splice region, to calculate shear stress developed in the concrete and predict if yielding of reinforcement is achieved. The accuracy of the analytical method was checked against experimental results from both the literature and the experimental work included herein.

Keywords: lap splices; bond-slip; retrofit; steel jacket; RC jacket

1. Introduction

Experience from strong earthquake events of the last forty years revealed numerous typical structural deficiencies of existing pre1960-70s reinforced concrete (RC) framed structures, related to brittle hysteretic response and catastrophic collapse. The seismic behaviour of columns and beam-column joints, which are members of the vertical bearing system, was recognized as a significant factor that frequently becomes critical for the overall seismic performance. Moreover, the existing RC structures often exhibit severe damaging of columns, resulting in the formation of soft storey mechanism with catastrophic effects. One of the most crucial factors related to this extremely dangerous and undesirable brittle failure mode is the inadequate length of the column lap-spliced reinforcing bars. In particular, lap splices of RC structures built prior to the 1970s were designed for gravity loads only, with a short length which is insufficient to ensure load transfer between the bars under tension. Furthermore, lap splices were located in the column critical region just above the floor slab, inside the potential plastic hinge region. Therefore, early loss of the bond between concrete and steel reinforcement occurs during a few cycles of lateral displacements caused by seismic excitations, followed by failure of the load transfer mechanism between lap-spliced reinforcement and excessive bar slipping. Accordingly, the overall hysteresis of the column is significantly affected, showing inability to develop the column nominal moment flexural capacity, rapid strength and stiffness deterioration, poor energy dissipation capacity and low ductility. Moreover, other typical co-existing structural inadequacies of existing RC structures, for instance low confinement of the column critical region, the use of plain steel bars and the use of low compression strength concrete, cause further degradation of the columns' seismic performance. Therefore, the latter are exceptionally susceptible to collapse under gravity loads, due to the loss of axial load carrying capacity. Meanwhile, the overall structural integrity and the safety of residents are seriously jeopardized.

Given the devastating influence of deficient column lap splices in the seismic performance of existing RC structures, it is absolutely necessary and imminent to improve the load transfer mechanism between the spliced reinforcement. Hence, reliable earthquake-resistant rehabilitation strategies and strengthening schemes have to be applied, to ensure that the seismic behaviour of the strengthened columns would be equally satisfactory with that of columns found in modern RC structures. Valuable knowledge on the influence of deficient lap splices to the

*Corresponding author, Professor
E-mail: tsonosa@civil.auth.gr
[a]Ph.D.
E-mail: geokal@civil.auth.gr

http://www.techno-press.com/journals/eas&subpage=7 ISSN: 2092-7614 (Print), 2092-7622 (Online)

column seismic performance was provided by the experimental and analytical investigation, conducted during the last thirty years. Thus, modern design Codes introduce the design of lap splices as tensile ones (EC2 and EC8, ACI-318). It was also demonstrated that the premature lap splice failure and restriction of bar slipping may be achieved mainly by providing adequate confinement to the column critical region, where lap splices are located.

Various retrofit schemes found in literature were developed to improve the hysteresis of columns found in pre-1970s RC structures. For instance, the shear strength, energy dissipation capacity and ductility may be significantly increased by fibre reinforced polymer (FRP)-wrapping or steel jacketing of the column critical region. Also, the RC jacketing causes changes of the column geometry, with additional beneficial effects to the lateral strength and stiffness of the strengthened column.

Rodriguez and Park (1994) experimentally investigated the seismic behavior of four column specimens with inadequate transverse reinforcement. The main variable examined was the amount of transverse reinforcement of the applied RC jackets. Test results revealed that the strengthened columns showed significantly improved lateral performance with respect to the original specimens, while also exhibited a ductile failure mode. In the experimental work of Julio and Branco (2008), the influence of interface treatment between the existing column and the RC jacket on the seismic behaviour was examined. Tsonos (2008) experimentally investigated the effectiveness of pre-earthquake and post-earthquake retrofit schemes in improving the overall hysteresis of beam-column joint subassemblages. Both conventional RC jacketing and innovative high strength steel fiber-reinforced concrete (HSFC) jacketing schemes were examined. The RC jacketing was found to be more effective for the post-earthquake strengthening procedure, while both retrofit schemes were found to be equally satisfactory for the pre-earthquake strengthening of the subassemblages. Hamilton *et al.* (2004) examined the effectiveness of shotcrete jacketing and RC jacketing in improving the shear strength of RC bridge columns. The efficiency of shotcrete jacketing and RC jacketing in improving the flexural and shear strength of beam-column joint subassemblages was also studied by Tsonos (2010). Kalogeropoulos and Tsonos (2014) investigated the effectiveness of a retrofit scheme, which combined the welding of lap-spliced column reinforcement with the RC jacketing of the column. The experimental results clearly demonstrated that the strengthened subassemblages achieved an indisputable superiority in their overall hysteretic behaviour with respect to the original columns, while also exhibiting a ductile failure mode. Karayannis *et al.* (2008) used local thin RC jackets for the post-earthquake strengthening of earthquake-damaged beam-column joint subassemblages. The enhanced specimens were subjected to the same lateral displacement history as the original ones and showed a desirable ductile behaviour. In the experimental work of Chalioris *et al.* (2008) it was clearly demonstrated that the use of thin RC jackets in the beam-column joint region and in the beam critical region significantly improves the seismic response and energy dissipation capacity, while also retains the geometry, mass and dynamic characteristics of the structure. In the experimental and analytical research of Kalogeropoulos *et al.* (2016), the efficiency of RC jacketing in improving the seismic performance of beam-column joint subassemblages found in pre-1970s RC buildings was evaluated. The test results indicated that if the deficient straight anchorage of the beam longitudinal reinforcement in the joint region is restored, then both the pre-earthquake and post-earthquake strengthened beam-column joint specimens show a substantial improvement in their overall lateral performance with respect to the original subassemblage. Otherwise, the strengthened specimens exhibit premature brittle pullout failure, identical to that of the original subassemblage.

A retrofit scheme equally effective as that of RC jacketing, cost-effective and with less intensive time and labour demands, includes the use of steel fiber-reinforced concrete for the construction of the jacket. Henager (1977) successfully replaced the transverse reinforcement of the beam-column joint region and part of the transverse reinforcement of the column and beam critical regions, using steel fiber volume fraction equal to 1.67 percent. As a result, a reduction of 50 percent in construction cost was achieved. A relatively new method, SIMCON (Slurry Infiltrated Mat Concrete), which is highly efficient in earthquake-resistant rehabilitation applications, was developed by Hackman *et al.* (1992). According to an innovative strengthening technique proposed by Tsonos (2007b) (patent No 1005657/2007), a non-shrink, non-segregating, rheoplastic steel fiber-reinforced concrete jacket of ultra-high performance (UHPSFC) was used without conventional reinforcement to strengthen and effectively improve the seismic behaviour of existing RC structures with poor reinforcement details. In a related research of Tsonos (2014), the seismic performance of beam-column joint subassemblages, strengthened with the aforementioned innovative high performance steel fiber-reinforced concrete (HPSFC) jackets, showed a substantial superiority compared to that of specimens enhanced with conventional RC jackets and primarily with FRP jackets. The efficiency of HPSFC jacketing in improving the seismic behaviour of pre-1970s RC bridge columns was also experimentally investigated by Tsonos *et al.* (2017).

Steel jacketing and composite material jacketing of columns may provide adequate confinement to the critical region, when the primary concerns of the earthquake rehabilitation strategies are the increase of the column ductility and energy dissipation capacity. Meanwhile, the column flexural strength and stiffness show minor increase, since the column geometry remains almost unchanged. Moreover, if lap splices of reinforcement are located in the potential plastic hinge region of the column, the confinement provided by steel or FRP jackets may prevent premature bond-slip failure and allow yielding of reinforcement. Hence, the column nominal flexural moment capacity would be developed. Nevertheless, steel and composite material jacketing demonstrate significant disadvantages. The most crucial disadvantage is the inability to effectively enhance the beam-column joint region, which may result in the collapse of the strengthened structure during future earthquake events (Paulay and Priestley 1992). Seismic tests conducted by Chai *et al.* (1991) on six large scale column specimens showed that columns strengthened by steel jackets achieved a ductile behaviour equivalent to that of columns found in modern RC structures. Moreover, the confinement provided by the jackets successfully prevented the premature failure of lap splices. Aboutaha *et al.* (1999) examined the effectiveness of rectangular steel jackets and steel cages in improving the seismic behaviour of columns with inadequate shear strength. Daudey and Filliatraut (2000) used five bridge pier specimens of 1:3.65 scale with typical reinforcement details of RC structures built before the 1970s. One specimen was used as the original one, while the other four were strengthened by steel jacketing. The main parameters studied were the geometry of the jacket, the distance between the jacket and the foundation and the properties of the filling material used in the gap between the jacket and the existing column. The cyclic response of RC columns strengthened by steel jackets and carbon fibre reinforced polymer (CFRP) jackets was examined by El Gawady *et al.* (2010). Choi *et al.* (2013) investigated the improvement in bond between concrete and steel bars when steel jackets were used to confine columns of circular cross-section. In the experimental study of Saadatmanesh *et al.* (1997) earthquake-damaged column specimens were strengthened with FRP jackets and exhibited more stable hysteresis loops with lower stiffness degradation ratio compared to the original columns. Moreover, the enhanced columns successfully developed their nominal flexural moment capacity and displacement ductility. Pavese *et al.* (2004) used composite material jackets to improve the behaviour of circular bridge piers subjected to inelastic cyclic lateral deformations. The original subassemblages had low shear strength, poor ductility and deficient lap splices of reinforcement, located at the potential plastic hinge region. In a relatively new analytical and experimental study, Pampanin *et al.* (2007) used CFRP laminates to strengthen existing poorly detailed RC buildings of the 1950-70s period, designed for gravity loads only. Typical structural deficiencies of these structures were related to the absence of confinement of the beam-column joint region, inadequate lap splices of the column reinforcement and anchorage of the beam bars in the joint region with endhooks. The exterior CFRP strengthened subassemblages showed desirable ductile and dissipating hysteresis behaviour with the formation of the plastic hinges in the beam, while the interior joints exhibited acceptable and controlled minor cracking in the joint panel zone. A partial retrofitting strategy using CFRP laminates was adopted in the case of the three-storey three-bay frame structure, which proved to be very satisfactory in improving the lateral behaviour and preventing brittle failure of the exterior joints and the formation of soft-storey mechanism. The use of CFRP sheets for the strengthening of circular and hollow rectangular cross-section RC bridge columns with low shear strength was examined by Yeh and Mo (2005). Karayannis and Sirkelis (2008) investigated the seismic performance of beam-column joint specimens strengthened with a combination of epoxy resin injections and CFRP plastics sheets. The retrofitted subassemblages showed a substantial improvement in the overall lateral behaviour with respect to the original columns. A new category of FRP products, super laminates, was recently used for the production of seamless shells around existing columns (Ehsani 2010).

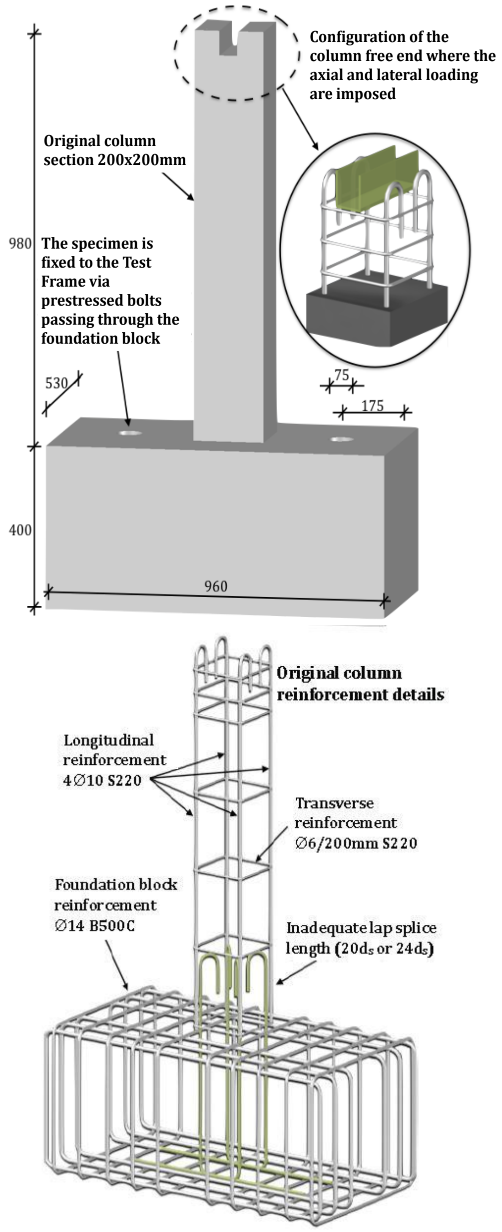

Fig. 1 Dimensions (mm) and reinforcement details of specimens O_1, O_2, G_1, G_2, E_1, E_2, N_1 and N_2

During the implementation of earthquake resistant rehabilitation strategies, the improvement of load transfer mechanism between the column lap-spliced reinforcement is usually underestimated. Nevertheless, the lap splice failures are related to extremely dangerous brittle response and catastrophic collapses. Thus, further investigation is required to evaluate the reliability and effectiveness of the aforementioned strengthening schemes in preventing the premature failure of lap splices during the incremental lateral displacement amplitudes of the seismic loading.

Table 1 Experimental program - Original and strengthened subassemblages

Series I - (C_1: control specimen, O_1, O_2: original specimens, SG_1, SG_2, SE_1, SE_2: pre-earthquake strengthened specimens)							
Original specimens					**Strengthened specimens**		
Specimen	Lap splice length (mm)	Longitudinal reinforcement	Transverse reinforcement	f'_c (Mpa)	Specimen	Steel jacket width d (mm)	Steel jacket length l_j (mm)
C_1*	Continuous bars			10.25	-	-	-
O_1*	$20d_s = 200$		∅6 mm ties (plain steel bars) 90° hook-ends, spaced at 200mm, $f_{ywd} = 263.5MPa$	9.81	-	-	-
O_2*	$24d_s = 240$	4∅10 mm plain steel bars, $f_{yd} = 374MPa$		8.80	-	-	-
G_1	$20d_s = 200$			8.51	SG$_1$*	1.0	
G_2	$24d_s = 240$			10.65	SG$_2$*	1.0	$max\begin{Bmatrix} l_{cr} \\ 1.30 \cdot l_s \\ 600mm \end{Bmatrix}$
E_1	$20d_s = 200$			9.04	SE$_1$*	5.0	
E_2	$24d_s = 240$			8.93	SE$_2$*	5.0	

Series II - (RC_2, RHN_1, RHN_2: pre-earthquake strengthened specimens)				
Original specimens (Not subjected to cyclic lateral displacements)				
Specimen	Lap splice length (mm)	Longitudinal reinforcement	Transverse reinforcement	f'_c (Mpa)
C$_2$	Continuous bars	4∅10 mm plain steel bars, f_{yd}=374 MPa	∅6mm ties (plain steel bars), 90° hook-ends, spaced at 200 mm, f_{ywd}=263.5 MPa	8.94
N$_1$	$20d_s = 200$			9.63
N$_2$	$24d_s = 240$			8.65

Strengthened specimens (Subjected to cyclic lateral displacements)				
Specimen	Longitudinal reinforcement of the RC jacket	Transverse reinforcement of the RC jacket	$f_{c,jacket}$ (Mpa)	Additional ties used to prevent lap splice failure
RC$_2$*	4∅10 mm B500C, f_{yd}=518 MPa	∅8 mm ties B500C with 135° hook-ends, spaced at 80 mm, f_{ywd}=518 MPa	60	-
RHN$_1$*				∅8/50 mm with 135° hook-ends, spaced at 80 mm, f_{ywd}=518 MPa
RHN$_2$*				

*Column subassemblages subjected to cyclic lateral displacements, representing the equivalent of strong earthquakes

2. Experimental program-strengthening interventions

Despite the wealth of experimental research on the retrofitting of columns and beam-column joint structural members, the research relating to the improvement of the cyclic behaviour of lap-spliced column reinforcement is rather poor. The strengthening schemes examined herein include thin steel jacketing or RC jacketing of columns found in structures built prior to the 1970s with poor reinforcement details and primarily with short and inadequate lap splices of reinforcement. Particular emphasis was given to reliably determining the confinement demand for ensuring premature lap splice failure prevention. Thus, an extensive experimental program was conducted on ten cantilever column subassemblages of 1:1.5 scale.

The first series of specimens (series I) included seismic tests on seven columns, while the main parameters examined were the lap splice length and the steel jacket width. Three identical pairs of original column subassemblages (O_1-O_2, G_1-G_2 and E_1-E_2), with poor reinforcement details typical of pre-1970s RC structures, were designed and constructed (see Table 1). Dimensions and cross-sections details of the specimens of series I are shown in Fig. 1. The original specimens had plain steel reinforcement S220, concrete of low compression strength C8/10 and widely spaced transverse reinforcement, consisted of ties with ninety-degree hook ends spaced at 200 mm. The concrete compression strength of the specimens was measured by using 150×300 mm cylinder compression tests (see Table 1). The length of lap splices equaled to twenty times (200 mm) and to twenty-four times the bar diameter (240 mm) in the case of columns O_1, G_1, E_1 and O_2, G_2, E_2, respectively. Using the appropriate equipment, the surface of subassemblages G_1, E_1, G_2 and E_2 was roughened, while the column edges were curved to allow improved confinement of the bars in the corners by the steel jacket. The radius of edge curvature equaled to two and a half times the width of the concrete cover (Chai *et al.* 1991) (see Fig. 2(a)). Subsequently, the column surfaces were cleaned with air pressure and covered in epoxy resin. Eventually, the two parts of the thin steel jacket were applied to the column and firmly attached using formwork clamps (see Figs. 2(b)-(c)). After seven days the epoxy resin reached its maximum strength and the two parts of each jacket were welded using two steel segments of the same width. Each steel jacket ended 2 cm above the foundation of the specimens. The strengthened columns were designated SG_1, SG_2, SE_1 and SE_2, respectively. The seismic behaviour of the retrofitted column specimens was compared with the hysteresis loops of the two original subassemblages with inadequate lap splices, O_1 and O_2 and a similar control specimen, C_1, with continuous longitudinal reinforcement.

The second series of subassemblages (series II) included three as-built columns, C_2, N_1 and N_2, identical to specimens C_1, O_1 and O_2, respectively. Using a jackhammer, the concrete cover of C_2, N_1 and N_2 was chipped away. Subsequently, the as-built columns were pre-earthquake strengthened with RC jackets, according to the provisions of Eurocode 2 and 8. However, in the case of N$_1$ and N$_2$ the confinement demand to prevent premature lap splice failure and excessive bar slipping during the cyclic loading was estimated. Thus, additional transverse reinforcement in the form of closed ties was used to confine the critical region of the existing columns N_1 and N_2, prior

(a) The surface was roughened and the edges were curved

(b) Epoxy resin was used to cover the column surface

(c) The parts of the jacket were firmly attached with formwork clamps

Fig. 2 Pre-earthquake strengthening process - Series I

Table 2 Strengthening scheme and cross-section dimensions of the subassemblages

Original specimens	Retrofitted specimens	Retrofit scheme	Cross-section dimensions (mm) of the columns
C_1	-	-	200x200
O_1	-	-	
O_2	-	-	
G_1	SG_1	Steel jacketing	
G_2	SG_2		
E_1	SE_1		
E_2	SE_2		
C_2	RC_2	RC jacketing	300x300
N_1	RHN_1*		
N_2	RHN_2*		

*Additional ties which were not part of the RC jacket transverse reinforcement were used to prevent premature lap splice failure

to the construction of the RC jacket (see Fig. 3 and Tables 1 and 2). These ties were not part of the jacket's transverse reinforcement and were placed in contact with the existing column as shown in Fig. 3. B500C steel bars of 8mm diameter were used to confine the existing column. The ⊔-shaped bars were placed in contact with the existing columns N_1 and N_2 and were suitably bent to form close hoops. The ends of the hoops were welded, according to the requirements of the Code for Steel Reinforcement Technology for Concrete (CSRTC 2008). Afterwards, four holes were drilled in the concrete of the foundation block of each specimen at appropriate positions and cleaned with air pressure. The longitudinal B500C steel bars of the RC jacket were inserted into the holes, while a flowable, non-shrinking epoxy resin was inserted inside the holes with a syringe, to ensure bonding between concrete and the jacket reinforcement. Connection between the longitudinal reinforcement of the RC jackets and the bars of the original columns was achieved with s-shaped steel segments which were welded to the bars (see Fig. 3) according to the provisions of the CSRTC (2008). The transverse reinforcement of the jackets consisted of B500C 8mm diameter deformed closed ties with welded ends. A premixed, non-shrink, rheoplastic, flowable, and non-segregating cement of high strength was used for constructing the cement grout jacket of the specimens.

3. Design of the strengthening schemes

The seismic response of RC columns with inadequate and extremely short lap splices of reinforcement is dominated by excessive bar slipping, due to the premature bond-slip failure. Eventually, the columns are susceptible to collapse under gravity load prior to the development of the flexural nominal moment capacity and before the exhaustion of the column shear strength. To prevent premature lap splice failure and ensure yielding of reinforcement, adequate confinement should be provided to the column critical region, where lap splices are located. Thus, the strengthening scheme applied to the columns of series I included the use of thin steel jackets, designed according to the provisions of the Greek Code for Interventions (GCI 2017). The latter introduces two expressions for calculating the required width of the steel jacket, Eqs. (1) and (2). Eq. (2) is actually a simplified form of Eq. (1), while it is used especially for steel jackets. Eq. (1) is used for both FRP and steel jackets. Both equations were subsequently evaluated. According to Eq. (1) the required width, t_j, of the continuous steel jacket was calculated equal to 1mm, while the corresponding value according to Eq. (2) equaled to 5 mm. Thus, a thin steel jacket of 1mm width was applied to the columns G_1 and G_2 with lap splices of length equal to twenty and twenty-four times the bar diameter, respectively. The corresponding identical specimens E_1 and E_2 were strengthened by a steel jacket of 5mm width (see Table 1).

$$\frac{A_j}{s_w d_s} = \frac{t_j}{d_s} = 1{,}3\left\{\left[\frac{\left(\frac{f_{sy}}{f_c}\right)}{\left[\left(2{,}2\frac{s}{s_u}+0{,}25\right)\left(\frac{l_s}{d_s}\right)\right]} -0{,}2\left(2\frac{c}{d_s}++1{,}5\right)\right]^2\right\}/\left(\frac{w}{d_s}\frac{E_j}{f_c}\frac{f_{ctm}}{f_c}\right) \quad (1)$$

$$t_j = 2\sqrt{2}\frac{E_j f_{ctm}}{\left(f'_{sy}\right)^2}w \quad (2)$$

$$\frac{A_j}{s_w} = t_j = \gamma_{Rd}\cdot\frac{(1-\lambda_s)}{\beta}\cdot\frac{1}{\mu}\cdot\frac{f_{yk}}{\sigma_{jd}}\cdot\frac{A_b}{l_s} \quad (3)$$

In Eqs. (1)-(3) t_j is the width of the steel jacket; A_j is the cross-section area of the jacket; s_w is the distance between stirrups or FRP strips; d_s is the diameter of the lap-spliced bars; f_c is the characteristic concrete strength; $f_{sy} = f_{yk}$ is the yield stress of the plain lap-spliced bars; l_s is the lap splice length; c is the concrete cover; E_j is the modulus of elasticity of the steel jacket equal to 210 GPa; f_{ctm} is the mean tensile strength of the concrete equal to $f_{ctm} = 0.3\cdot f_{ck}^{2/3} = 1.2$ MPa; f'_{sy} is the yield stress of the steel jacket, which was determined equal to $f'_{sy} = 227.5$MPa through experimental tensile tests on three specimens; w is the dilation of the concrete cracking between the column lap-spliced bars equal to $w = 0.33$ mm, which corresponds to the maximum accepted value of relative slipping, $s = 0.4$ mm, according to the GCI; $s_u = 2$ mm is the critical friction slippage; γ_{Rd}, λ_s,

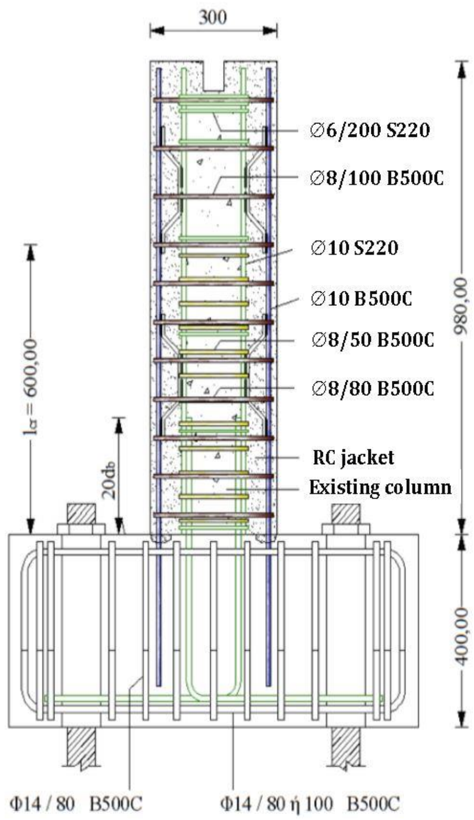

Fig. 3 Retrofit interventions - series II. Reinforcement of the RC jacket and additional ties (∅8/50 mm) used for improving the seismic response of the lap splices (columns RHN_1 and RHN_2)

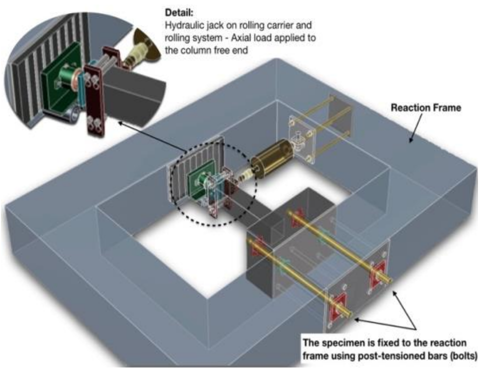

(a) Aerial view of the test setup

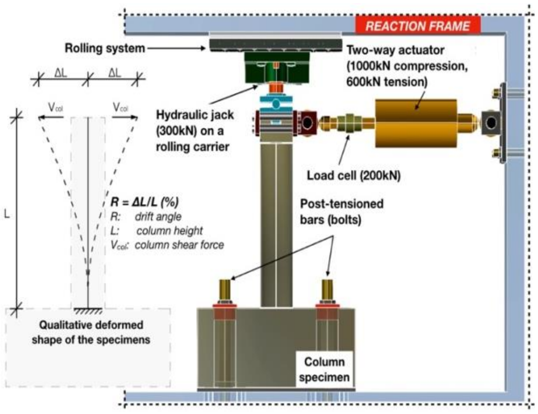

(b) Details of the reaction frame and the instrumentation used

Fig. 4 Test setup and qualitative deformed shape of the specimens

β and μ are coefficients equal to 1.5, 0, 1.0 and 1.0, respectively according to GCI; $\sigma_{jd} = E \cdot \varepsilon_{jd}$ is the design stress which is equal to the yield stress $\sigma_{jd,max} = f_y = 500/1.5 = 435\text{MPa}$ for the additional B500C closed hoops used to improve the load transfer mechanism between the lap-spliced bars; A_b is the diameter of one lap-spliced bar.

The column subasemblages of series II were retrofitted by RC jacketing, while designed to conform to the provisions of Eurocode 2 and 8. However, prior to the construction of the RC jacket additional closed ties were placed in contact with the existing column along the critical height, after the concrete cover was chipped away (see Fig. 3). The additional ties were calculated according to the GCI (Eq. (3)) and they were particularly used to provide adequate confinement to the lap splices and ensure yielding of the lap-spliced reinforcement.

Eq. (5) was used to control the concrete compression strut adequacy of the RC jacket. In Fig. 3 the Eurocode provisions for the required column shear reinforcement are presented. The transverse reinforcement demand for the RC jacket was finally determined using Eq. (6), where it is recommended that $V_{Rd,s} \geq V_{sd}$. In Eqs. (4)-(6) $A_{s,ex}$ is the cross-section area of the existing column; $A_{s,j}$ is the cross-section area of the RC jacket; $f_{ck,ex}$ is the concrete characteristic strength of the existing column; $f_{ck,j}$ is the concrete characteristic strength of the RC jacket; f'_{ck} is the equivalent concrete characteristic strength of the retrofitted column; $V_{Rd,max}$ is the strength of the concrete compression struts; $V_{Rd,s}$ is the shear force resisted by the hoops; A_{sw} is the cross-section area of the transverse reinforcement; s is the spacing of the stirrups; f_{ywd} is the yield strength of the transverse reinforcement; b_w is the cross-sectional depth of the column; $z = 0.9 \cdot d$; a_{cw} is a coefficient taking account of the state of the stress in the compression strut; v_1 is the strength reduction factor for concrete cracked in shear with recommended value of $1 - f_{ck}(\text{MPa})/250$ and θ is the angle between the concrete compression strut and the member axis perpendicular to the shear force $(\theta = 22°)$. Ultimately closed B500C ties of 8mm diameter spaced at 80mm were placed along the critical height of the strengthened column subassemblages. The cross-section dimensions of the original and strengthened columns of series II are shown in Table 2.

$$(A_{s,ex} \cdot f_{ck,ex} + A_{s,j} \cdot f_{ck,j})/(A_{s,ex} + A_{s,j}) = f'_{ck} \tag{4}$$

$$V_{Rd,max} = a_{cw} \cdot b_w \cdot z \cdot v_1 \cdot f_{cd}/(\cot\theta + \tan\theta) \tag{5}$$

$$V_{Rd,s} = (A_{sw}/s) \cdot z \cdot f_{ywd} \cdot \cot\theta \geq V_{sd} \tag{6}$$

4. Test setup and displacement history

The original and the retrofitted subassemblages were

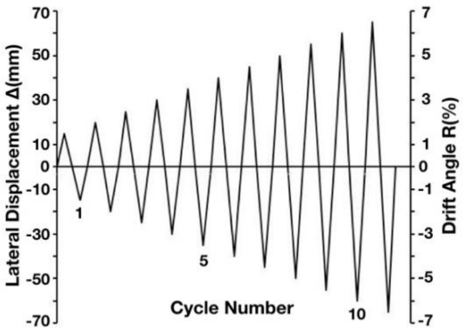

Fig. 5 Lateral displacement history

subjected to a large number of inelastic cycles of lateral displacement to simulate the equivalent effect of strong earthquakes. The columns were loaded transversely, under constant axial loading of 150 kN. The seismic tests were conducted in the test setup shown in Fig. 4, which is located in the Laboratory of Reinforced Concrete and Masonry Structures of the Aristotle University of Thessaloniki. The structures were fixed to the test frame with post-tensioned bars (bolts), thus the horizontal and vertical displacement and the rotation of the foundation block of each column were restrained. A hydraulic jack, placed on top of each

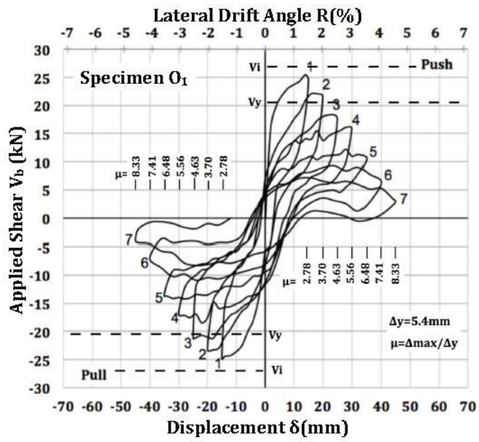

(a) Hysteresis loops of the original specimen, O_1

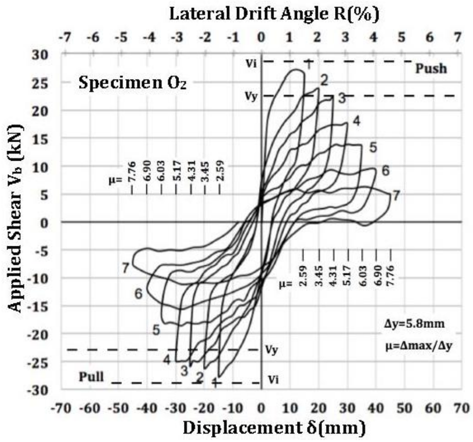

(b) Hysteresis loops of the original specimen, O_2

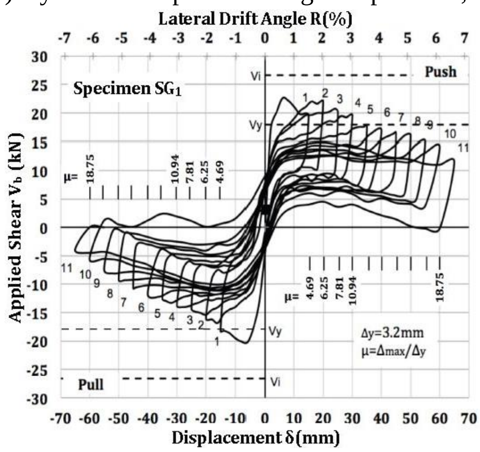

(c) Hysteresis loops of the strengthened specimen, SG_1

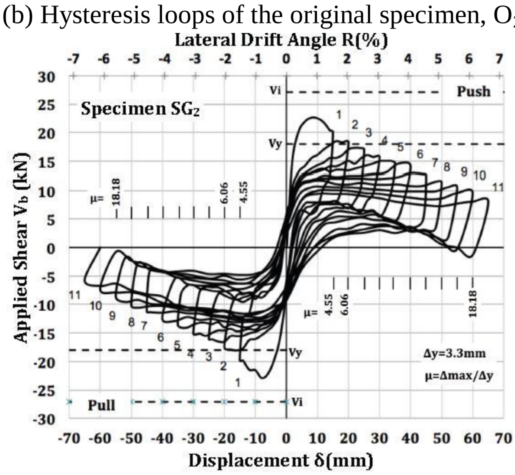

(d) Hysteresis loops of the strengthened specimen, SG_2

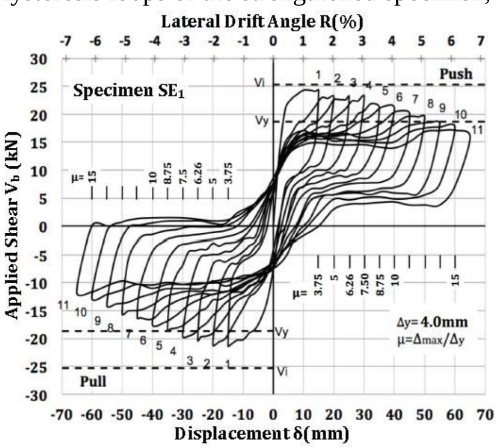

(e) Hysteresis loops of the strengthened specimen, SE_1

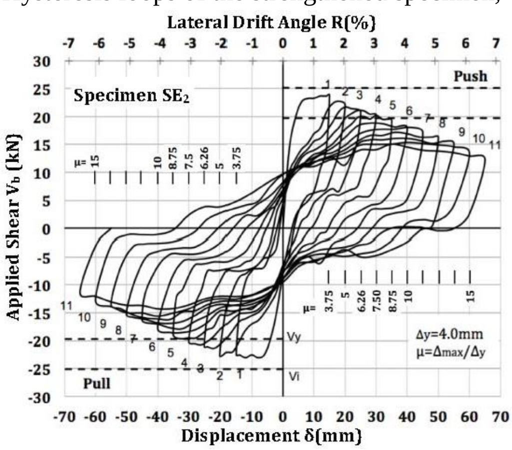

(f) Hysteresis loops of the strengthened specimen, SE_2

Fig. 6 Plots of applied shear-versus-displacement of the original specimens column perpendicular to the lateral loading direction, was used to impose the axial load on the specimens and was controlled to remain constant during the tests. The lateral loading was applied using a two-way actuator by slowly displacing the column free end of the specimens. The shear resistance of the columns was measured by a load-cell, while a calibrated linear variable differential transducer was used to control the load point displacement. Electrical resistant strain gages were installed on the columns' longitudinal and transverse reinforcement to measure the steel strain values during the seismic loading and ascertain the yielding of reinforcement.

All specimens were loaded transversely following the displacement-controlled schedule shown in Fig. 5. The seismic loading sequence was established to capture critical issues of the element capacity, for instance the ultimate limit state of the column. Given that the inelastic cyclic deformations cause cumulative damage and that the behaviour of subassemblages is mainly demonstrated by the envelope curves, a loading sequence with constantly increasing lateral displacement per step and with one cycle per amplitude of displacement was adopted, without considerable influence in the seismic performance of the subassemblages. An original specimen was used to determine the steps of loading and was at first loaded to its yield displacement, after which significant decrease in stiffness occurs. This was measured from the plot of applied shear-versus-displacement of the specimen, while it was also verified by the yielding of the longitudinal column reinforcement using strain gages. The loading was continued in the same direction (push cycles) to 1.5 times the yield displacement and the subassemblage was subsequently unloaded and loaded in the other direction (pull cycles) to the same lateral displacement. After the first cycle of loading, the maximum displacement of each subsequent cycle was increased incrementally by 0.5 times the yield displacement (Hakuto *et al.* 2000, Ehsani and Wight 1985, Durani and Wight 1987).

5. Experimental results-interpretation of the failure mode

The overall seismic performance of the original and pre-earthquake strengthened column subassemblages of both series I and II is evaluated herein. For this purpose, the lateral strength, peak-to-peak stiffness and energy dissipation capacity of the specimens are compared. The seismic behaviour of the column subassemblages is clearly demonstrated in the hysteresis loops, illustrated in Figs. 6-7.

The column specimens of series I were designed with similar material properties and reinforcement details. Thus, given that the steel jackets stopped 20 mm over the foundation of the subassemblages and that the damage (main flexural crack) was formed in the column base, only slight differences of 3-4 kN in lateral strength of both the original and the strengthened columns were observed in the first cycle of seismic loading (see Fig. 6). However, during the consecutive cycles of inelastic lateral displacements applied to the column free end, all columns showed a reduction in lateral strength.

Due to the premature lap splice failure, the original specimens O_1 and O_2 exhibited rapid degradation of lateral strength, which was practically exhausted after 45 mm of reversed lateral displacement, resulting in the collapse of the columns. The strengthened column SE_1 showed slightly increased lateral strength with respect to the control specimen, C_1, for lateral drift ratio values higher than 2.55 and 3.06 percent in the push and pull half-cycles, respectively (see Figs. 6-7). The lateral strength of specimen SE_2 was also higher than that of columns C_1 and SE_1 in all pull half-cycles, while it was slightly reduced with respect to that of C_1 until the seventh push half-cycle. Subassemblages SG_1 and SG_2, strengthened with steel jacket of 1mm thickness, showed inferior lateral strength with respect to specimens SE_1, SE_2 and C_1 (see Figs. 6-7). Particularly, the mean strength ratio value SG_2/C_1 equaled to 0.73 in the push half-cycles, while the corresponding value for specimen SG_1 (SG_1/C_1) equaled to 0.71 in the case of pull half-cycles. Contrariwise, the lateral strength of specimens SE_1 and SE_2, strengthened with steel jacket of 5mm thickness, was similar or even higher than that of the control subassemblage, C_1. For instance, the strength ratio SE_1/C_1 equaled to 1.44 and 1.76 during the eleventh push and pull half-cycle, respectively. In the case of strength ratio SE_2/C_1 the corresponding values were equal to 1.10 and 1.72. For drift ratio of 4.59 percent the strength ratio values SG_1/O_1, SG_2/O_2, SE_1/O_1 and SE_2/O_2 for the push/pull half-cycles equaled to 4.85(push)/2.47(pull), 2.57/1.38, 6.04/3.79 and 3.71/2.07, respectively.

The cyclic loading also caused reduction of the peak-to-peak stiffness of all specimens. The observed stiffness deterioration ratio was higher for the original columns O_1 and O_2 than for the strengthened specimens, SG_1, SG_2, SE_1 and SE_2 and the control subassemblage, C_1. After eleven cycles of lateral loading the remained stiffness of the strengthened columns ranged from 7.29 (specimen SG_1) to 13.95 percent (specimen SE_1) of the corresponding values during the first cycle. For lateral drift ratio, R, of 4.59 percent the remained stiffness of the original columns O_1 and O_2 was minimal, while the specimens eventually collapsed due to the excessive damage and loss of axial load carrying capacity.

The strengthened specimens SE_1 and SE_2 showed increased stiffness compared to the control specimen, C_1, for drift ratio values higher than 2.55 and 4.08 percent, respectively (see Figs. 6-8). Moreover, the peak-to-peak stiffness of the enhanced columns SG_1 and SG_2 was higher than that of O_1 and O_2 for drift ratio values higher than 2.04 and 3.06 percent, respectively. During the seismic tests the stiffness of specimens SE_1 and SE_2 was superior to that of SG_1 and SG_2, while after eleven cycles of seismic loading SE_1 and SE_2 showed 57 and 34 percent higher stiffness values than that of the control specimen, C_1, respectively (see Fig. 8(a)). On the contrary, the retrofitted subassemblages SG_1 and SG_2 showed a mean stiffness value equal to 81 and 69 percent of the stiffness of C_1. Consequently, the small thickness of the steel jackets had only minor impact in the geometry of columns, thus, no substantial improvement in stiffness of the strengthened specimens was observed with respect to the stiffness of the original columns.

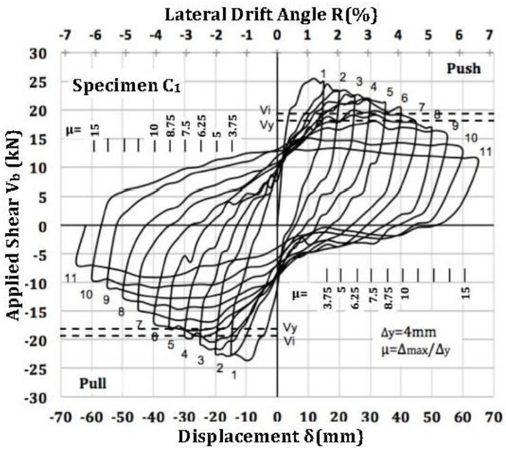

(a) Hysteresis loops of the control specimen of series I, C_1

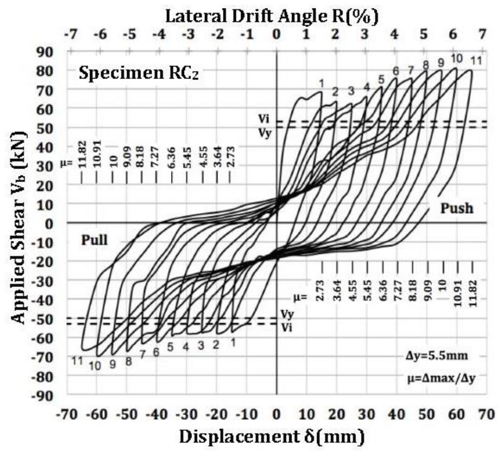

(b) Hysteresis loops of the control specimen of series II, RC_2

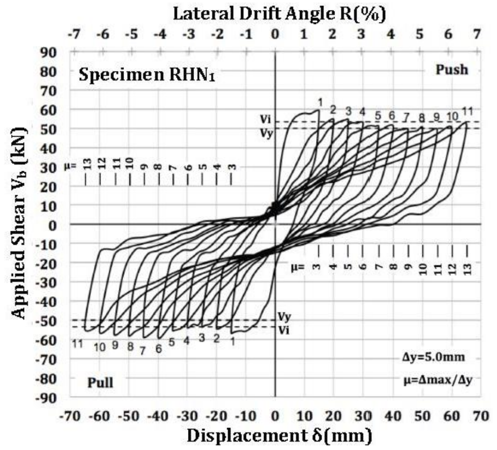

(c) Hysteresis loops of the strengthened specimen, RHN_1

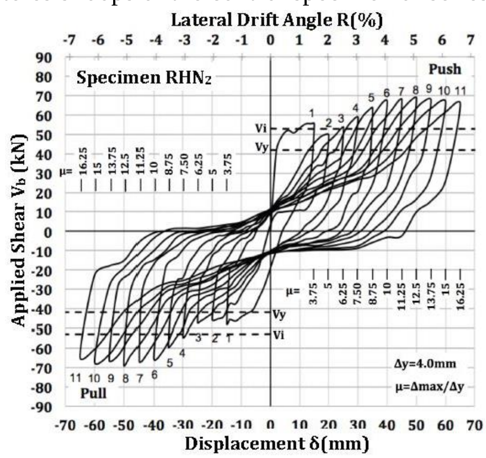

(d) Hysteresis loops of the strengthened specimen, RHN_2

Fig. 7 Plots of applied shear-versus-displacement of the strengthened specimens of series II and control specimens C_1, RC_2.

The confinement provided by the steel jacket of 1 mm thickness was inadequate to effectively improve the energy dissipation capacity of the strengthened subassemblages SG_1 and SG_2 (see Fig. 8(c)). The latter, exhibited excessive slipping of the lap-spliced reinforcement, while it also showed poor energy dissipation capacity, similar or inferior to that of the original columns O_1 and O_2 up to drift ratio values equal to 4.08 percent (specimen SG_1) and 4.59 percent (specimen SG_2), respectively.

For lateral displacement equal to 40 mm the energy dissipation ratios SG_1/O_1 and SG_2/O_2 equalled to 1.12 and 1.11, respectively. Moreover, the energy dissipation capacity of the enhanced columns SG_1 and SG_2 was significantly lower than that of the original column without lap splices of reinforcement, C_1. In particular, the energy dissipated in the plastic hinge of SG_1 and SG_2 was a mere portion of that dissipated by C_1, while at the end of the seismic tests the energy dissipation ratios SG_1/C_1 and SG_2/C_1 equalled to 0.53 and 0.46, respectively. Contrarily, the specimens strengthened with 5 mm thick steel jacket, SE_1 and SE_2, showed increased energy dissipation capacity with respect to columns SG_1 and SG_2. During the first cycle of the lateral loading subassemblage SE_2 dissipated almost 90 percent of the energy dissipated by the control specimen, C_1, while also achieved a 22 percent increase in the energy dissipation capacity with respect to specimen C_1 during the eleventh cycle of loading (see Figs. 6-8(c)). For drift ratio, R, equal to 4.59 percent the energy dissipation ratio values SE_1/O_1 and SE_2/O_2 equalled to 1.75 and 1.93, respectively. At the end of the seismic tests the energy dissipation ratio values SE_1/C_1, SE_2/C_1, SE_1/SG_1 and SE_2/SG_2 equalled to 0.77, 1.04, 1.13 and 1.82, respectively. The steel jacket successfully confined the critical region of subassemblages SE_1 and SE_2 where lap splices of reinforcement are located, allowing yielding of the lap-spliced bars. Moreover, the jacket prevented crushing of the concrete in the column compression zones and disintegration of the core concrete. As a result, unlike the control specimen, C_1, buckling of the longitudinal reinforcement of SE_1 and SE_2 under the column axial load was prevented. The restriction of bar slipping ensured increased dissipation of seismic energy in the plastic hinge of SE_1 and SE_2, while the latter, showed similar energy dissipation capacity with the control specimen without lap splices of reinforcement, C_1 (see Fig. 8(c)).

In Fig. 6 the hysteretic behaviour of the original and strengthened specimens of series I is presented. It is clearly demonstrated by the shape of the hysteresis loops that the inelastic cyclic performance of the columns is affected by P-Δ effect. The seismic response of the control specimen, C_1, which lacked lap splices of reinforcement, is noticeably less influenced by the P-Δ effect, with respect to the columns with lap-spliced bars. Meanwhile, the *P*-Δ effect had a great influence in the case of the strengthened subassemblages SG_1 and SG_2, due to the poor flexural strength of the columns and excessive bar slipping in the plastic hinge region. This is clearly reflected in the hysteresis loops of the enhanced with 1mm thick steel jacket specimens, SG_1 and SG_2 and also in the loops of specimen SE_1, strengthened with steel jacket of 5 mm thickness (see Fig. 6) In the latter, however, yielding of the lap-spliced column reinforcement was achieved. The restriction of bar slipping and the yielding of lap-spliced reinforcement resulted in a reduced impact of the *P*-Δ effect in the inelastic cyclic response of the strengthened column SE_2. Thus, the hysteresis loops of SE_2 were similar to the loops of the control specimen C_1.

The ductile failure mode of C_1 interprets the seismic behaviour of the control specimen, which was ideal for columns of existing pre-1960-70s RC structures due to the absence of lap splices.

The seismic response of the strengthened columns SG_1, SG_2, SE_1 and SE_2 was dominated by the *P*-Δ effect, especially in the case of SG_1 and SG_2. Specimen SE_2 exhibited a more ductile behaviour with respect to the other strengthened columns, which was very close to that of C_1.

The strengthening scheme applied to the subassemblages of series II effectively and substantially improved the behaviour of columns RHN_1 and RHN_2 during the consecutive cycles of inelastic lateral displacements. The latter, showed an indisputable superiority in the overall seismic performance with respect to the original specimens O_1 and O_2. The lateral strength of RC_2 and RHN_2 showed a gradual and continuous increase during the seismic tests (except for the second push half-cycle of loading). Specimen RHN_1 showed almost stable hysteresis, with high values of lateral strength until the end of the seismic loading. For drift ratio, *R*, of 6.63 percent the strength ratio RHN_1/RC_2 equalled to 0.66 for the push half-cycle and 0.83 for the pull half-cycle. From the envelope curves illustrated in Fig. 7 it can be observed that the change in lateral strength of RHN_2 is similar to that of the control specimen of series II, RC_2. At the end of the seismic tests (*R*=6.63 percent) the lateral strength ratio value RHN_2/RC_2 equalled to 0.834 and 0.991 for the push and pull half-cycle, respectively (see Fig. 7). The implementation of the retrofit measures also improved the lateral strength of specimens RHN_1 and RHN_2 exceptionally, compared to that of the original columns O_1 and O_2. In particular, during the first push half-cycle and pull half-cycle of the seismic loading, specimen RHN_1 showed 2.41 and 2.28 times the strength of the original column O_1, respectively. The corresponding values for subassemblage RHN_2 equalled to 2.12 and 1.72 times the strength of column O_2. At the end of the seventh cycle of loading, when the original columns O_1 and O_2 practically collapsed, the strengthened specimens RHN_1 and RHN_2 showed 14.50 (push half-cycle)/13.55 (pull half-cycle) and 13.94 (push half-cycle)/8.27 (pull half-cycle) times the strength of specimens O_1 and O_2, respectively.

Due to the construction of the RC jackets, a significant change in the geometry of the strengthened columns RC_2, RHN_1 and RHN_2 was achieved, with respect to the geometry of the initial columns, C_2, N_1 and N_2. As a result,

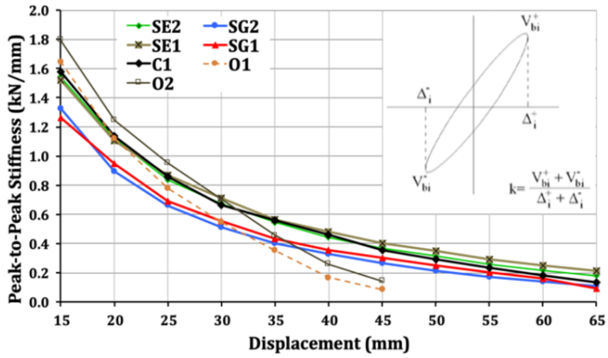

(a) Peak-to-peak stiffness - series I

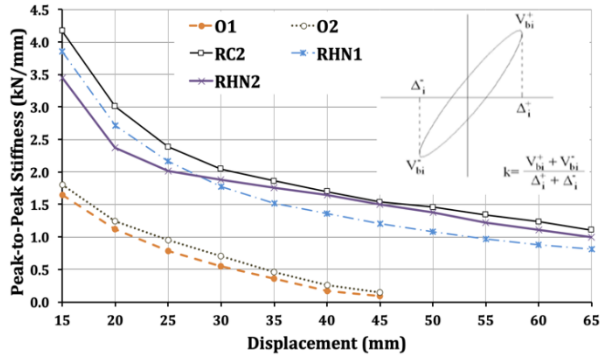

(b) Peak-to-peak stiffness - series II

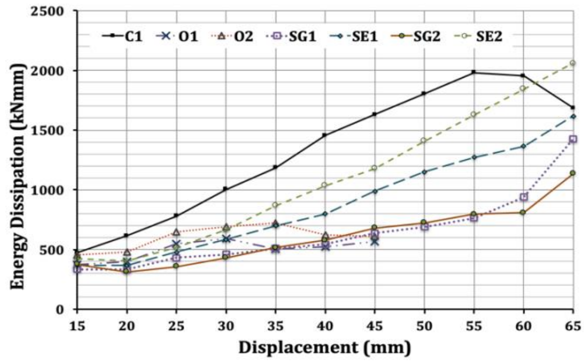

(c) Energy dissipation capacity - series I

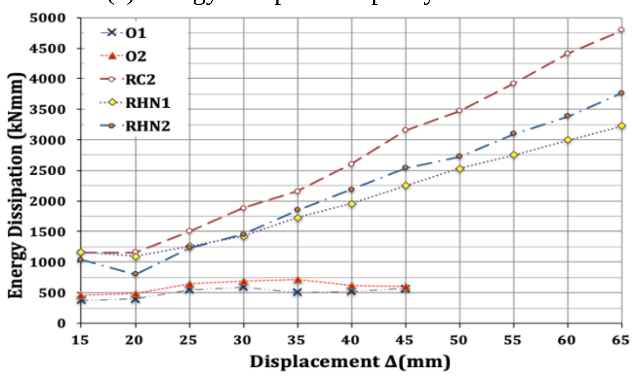

(d) Energy dissipation capacity - series II

Fig. 8 Peak-to-peak stiffness and energy dissipation capacity of specimens

the enhanced subassemblages RC_2, RHN_1 and RHN_2 showed a substantially increased peak-to-peak stiffness, compared to the original columns O_1 and O_2 (see Fig.8(b)). During the first cycle of the seismic loading, the peak-to-peak stiffness ratios RHN_1/O_1 and RHN_2/O_2 equalled to 2.34

and 1.92, while for lateral drift ratio, R, of 4.59 percent the corresponding values equalled to 13.95 and 10.71, respectively. The stiffness of column RHN_2 was similar to that of RC_2, while after eleven cycles of the seismic loading the stiffness ratio RHN_2/RC_2 equalled to 0.905.

The strengthened specimens RHN_1 and RHN_2 also showed a spectacular improvement in the energy dissipation capacity, compared to the original columns O_1 and O_2. Moreover, the values of energy dissipated in the plastic hinge of RHN_1 and RHN_2 were very close to these of the control specimen, RC_2 (see Fig. 8(d)). Up to a drift ratio, R, equal to 2.55 percent, specimen RHN_1 showed slightly increased energy dissipation capacity compared to subassemblage RHN_2. During the first cycle of loading the energy dissipation ratios RHN_1/RC_2, RHN_2/RC_2, RHN_1/O_1 and RHN_2/O_2 equalled to 0.673, 0.785, 3.12 and 2.29, respectively. After seven cycles of loading the original columns collapsed, while the energy dissipation ratio values RHN_1/O_1 and RHN_2/O_2 equalled to 3.97 and 4.17, respectively.

The hysteretic response of the strengthened specimens of series II is shown in Fig. 7. The spindle-shaped hysteresis loops of all specimens reflect the significantly increased energy dissipation capacity, while the absence of pinching around the axes and the continuous increase of lateral strength with the increase of lateral displacement, indicate the satisfactory restriction of bar slipping. Moreover, the influence of the P-Δ effect in the cyclic behaviour of the strengthened subassemblages RHN_1 and RHN_2 was minimal, due to the high strength of the enhanced columns. Furthermore, the inherent strength of the concrete (60MPa) and the strong confinement provided by the RC jacket, prevented the loss of the concrete cover and buckling of the longitudinal reinforcement. Meanwhile, yielding of the lap-spliced bars (found in the initial columns) and yielding of the longitudinal reinforcement of the RC jacket was achieved. Eventually, the specimens RHN_1 and RHN_2 exhibited a ductile failure mode, while the RC jackets of the columns remained intact at the end of the seismic tests (see Fig. 9(i)-(j)). Thus, it was clearly demonstrated from the experimental results that the strengthening scheme applied to the columns effectively improved the load transfer mechanism between the lap-spliced reinforcing bars and ensured the ductile seismic performance of the strengthened columns.

6. Steel micro-strain monitoring

Electrical resistant strain gages were used to measure the steel reinforcement strain of the original and strengthened subassemblages of series I and II. The seismic behaviour of the original specimens O_1 and O_2 and the performance of the strengthened columns SG_1 and SG_2 were dominated by excessive bar slipping, due to the premature failure of lap splices. Hence, minimal strain of the plain longitudinal bars was expected for the specimens. In particular, columns O_1, O_2, SG_1 and SG_2 performed poorly under the incremental displacement amplitudes of the lateral loading, while were unable to develop their nominal flexural moment capacity. On the contrary, the strain values

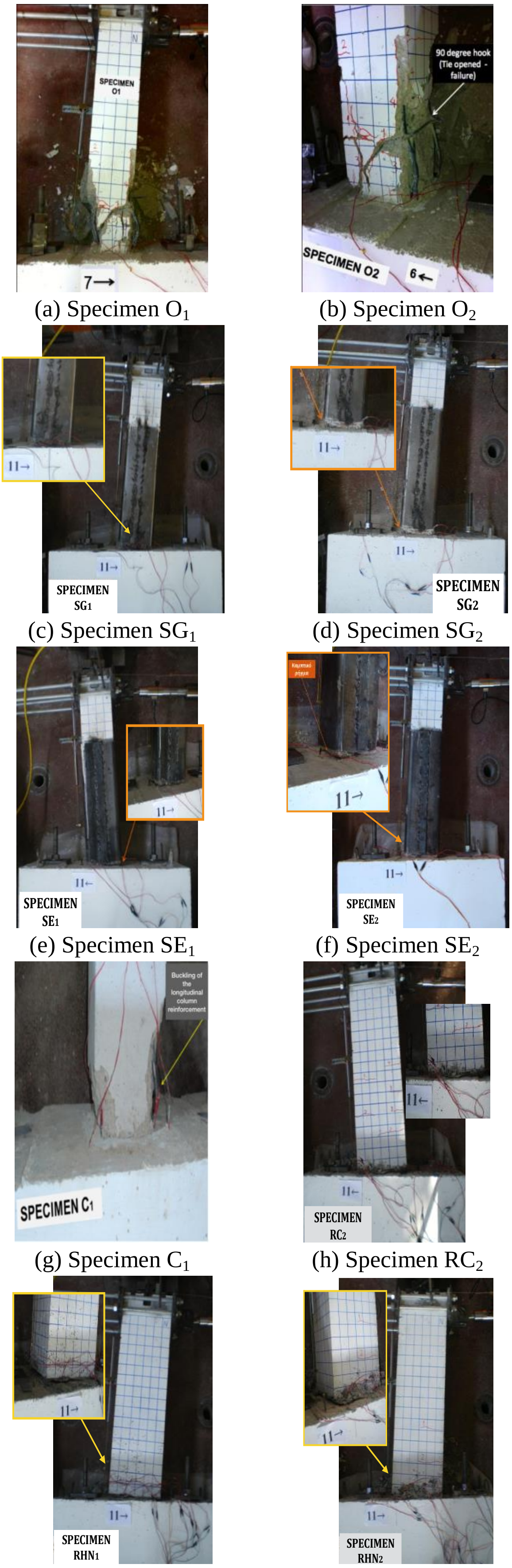

(a) Specimen O_1 (b) Specimen O_2
(c) Specimen SG_1 (d) Specimen SG_2
(e) Specimen SE_1 (f) Specimen SE_2
(g) Specimen C_1 (h) Specimen RC_2
(i) Specimen RHN_1 (j) Specimen RHN_2

Fig. 9 Failure mode of the original and strengthened specimens (a)-(g): series I, (h)-(j): series II of the lap-spliced reinforcing bars of the strengthened specimens SE_1 and SE_2 continually increased during the consecutive cycles of seismic loading and even exceeded the steel yield strain of 1.87‰. The measured maximum strain values for subassemblages O_1, O_2, SG_1, SG_2, SE_1, SE_2 equalled to 0.28‰, 0.42‰, 0.632‰, 0.998‰, 1.92‰, and 3.3‰, respectively.

According to Ehsani and Whight (1985) the continuous increase in maximum steel strain between two consecutive cycles of loading indicates the absence of bar slipping and ductile lateral response, while stable or decreasing strain values reflect hysteresis deterioration due to the slippage of the bars, as long as buckling has not taken place. Thus, the increase in strain values of SE_1 and SE_2 indicates that the confinement provided by the steel jacket successfully improved the load transferring mechanism between the lap-spliced bars and prevented the early failure of the short lap splices. Measures from the strain gages also showed that yielding of both the plain lap-spliced steel bars of the existing column and of the ribbed longitudinal reinforcement of the RC jacket was achieved, in the case of the strengthened columns of series II, RHN_1 and RHN_2. For instance, in the case of specimen RHN_1 the measured maximum strain value of the plain lap-spliced bar equaled to 2.03‰ and that of the ribbed longitudinal reinforcement of the RC jacket equaled to 2.60‰. The corresponding values for the strengthened column RHN_2 were 4.55‰ and 18‰, respectively. The continuous increase in steel strain, observed in specimens RHN_1 and RHN_2 reflects the effectiveness of the retrofitting technique in improving the load transfer between the deficiently lap-spliced bars. Therefore, it was clearly demonstrated that a significant superiority was achieved in the hysteretic behaviour of subassemblages RHN_1 and RHN_2 with respect to the original columns O_1 and O_2.

7. Theoretical considerations

Tsonos (2007a, 2019) proposed an analytical model for effectively preventing the collapse of RC buildings subjected to a large number of inelastic cyclic lateral displacements during strong seismic excitations. According to the formulation, the ultimate shear capacity of the beam-column joint region is computed and compared to the value of the connection shear stress for which yielding of the beam reinforcement is achieved. Thus, the model accurately predicts if the connection fails earlier than the beam(s) or not.

The aforementioned methodology was slightly modified to be applied and accurately predict the seismic behavior of an entirely different region. Therefore, the analytical model proposed herein is used to control adequacy of the lap splice length of columns found in both existing and modern RC structures. Moreover, the methodology is also applied during the earthquake resistant rehabilitation process of existing RC structures. In this case it is used to control adequacy of the confinement provided by the jacketing of columns for preventing early lap splice failure. Ultimately, the premature lap splice failure is prevented, while yielding of the lap-spliced reinforcement is also achieved by

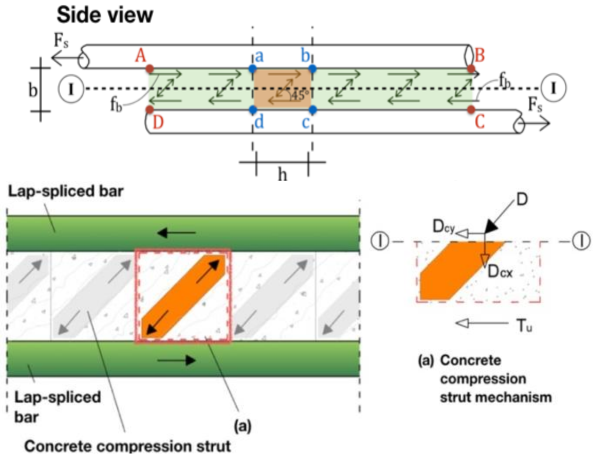

Fig.10 Forces acting in the lap splice region through section I-I from the concrete compression strut mechanism

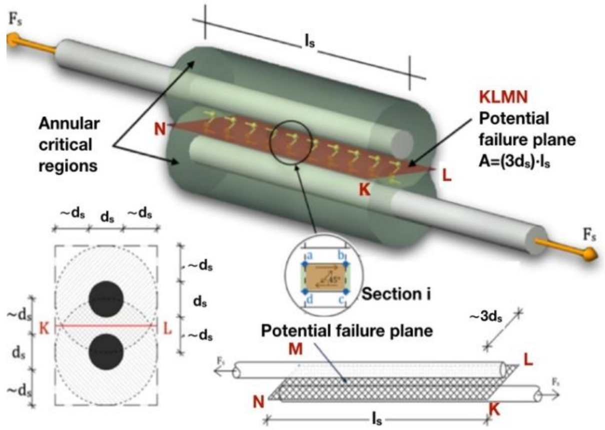

Fig. 11 Annular critical regions and potential failure plane

providing adequate confinement to the column critical region, where lap splices of reinforcement are located.

Fig. 10 shows the detail of lap-spliced reinforcement, which is located in the potential plastic hinge region of a RC column, just above the floor slab. During the seismic loading, tensile (and compressive) forces are developed in the lap-spliced bars, acting in opposite directions. Due to the bond between concrete and steel, bond stresses in the circumference of the bars cause diagonal compression of the concrete in every single section "*abcd*". These shear forces acting on 45 degrees angle (Paulay 1982) are resisted by compression struts that act between diagonally opposite corners of each rectangular section "*abcd*" (see Fig. 10). The mechanism of diagonal compression struts depends on the concrete strength. Thus, the ultimate concrete strength under compression/tension controls the ultimate strength of the lap splice. After the failure of concrete, strength in the lap splice is limited by gradual crushing along the cross - diagonal cracks and especially along the potential failure plane (see Fig. 11), while slipping of the bars occurs.

For instance, consider the section I - I in the middle of the lap splice height (see Fig. 10). For every single section, i (abcd), the forces acting in the concrete are shown in Fig. 10. Each force is analyzed into two components along the X and Y axes. Thus, the vertically acting force of section i (abcd) is $D_{cy} = V_{sp.v,i}$, while the horizontally acting force of section i is $D_{cx} = V_{sp.h,i}$. For uniform normal and shear stress distribution in section I - I, the sum of all $V_{sp.v,i}$ forces gives the vertical component of shear stress acting between the lap-spliced bars, $V_{sp.v}$, while the sum of all $V_{sp.h,i}$ forces gives the horizontal component $V_{sp.h}$ (Eqs.(7)-(8)).

$$V_{sp.v} = \sum_{i=1}^{v} V_{sp.v,i} = \left(V_{sp.v,1} + V_{sp.v,2} + \cdots + V_{sp.v,v}\right) \quad (7)$$

$$V_{sp.h} = \sum_{i=1}^{v} V_{sp.h,i} = \left(V_{sp.h,1} + V_{sp.h,2} + \cdots + V_{sp.h,v}\right) \quad (8)$$

The normal compressive stresss, σ and the shear stress, τ, uniformly distributed over the section I - I are given by Eqs. (9) and (10), respectively.

$$\sigma = \frac{V_{sp.h}}{A} \quad (9)$$

$$\tau = \frac{V_{sp.v}}{A} \quad (10)$$

According to literature (Paulay 1982) for each section "*abcd*" the aspect ratio $a = h/b$ is always equal to 1.0. Thus, by dividing Eqs. (9) and (10) the relation between the normal compressive stress, σ and the shear stress, τ, is established ($\sigma = \tau$), (Eq. (11)).

$$\frac{\sigma}{\tau} = \frac{V_{sp.h,i}}{V_{sp.v,i}} = \frac{b}{h} = a = 1.0 \quad (11)$$

It is now necessary to determine the dimensions of the potential failure plane *KLMN*, to calculate the ultimate strength of the concrete (see Fig. 11). The length of the failure plane, $(NK) = (ML)$, equals to the lap splice length, l_s, while the precise selection of the plane width, $(NM) = (KL)$, depends on the tensile strength of the concrete, σ_{ct}, perpendicular to the reinforcing bars. In particular, when the bond stress value in the circumference of the bar becomes equal to $2\sigma_{ct}$, splitting cracks are forming in the concrete perpendicular to the bar. As a result, an annular critical space is formed around each lap-spliced bar with diameter equal to three times the bar diameter, d_s and length equal to l_s. Consequently, the area of the potential failure plane equals to $A = 3 \cdot d_s \cdot l_s$.

The expression that gives the ultimate strength of the lap splice is the same with that of Tsonos model (Eq. (12)).

$$(x + \psi)^5 + 10\psi - 10x = 1 \quad (12)$$

where

$$x = \frac{\alpha\gamma}{2\sqrt{f_c}} \quad , \quad \psi = \frac{\alpha\gamma}{2\sqrt{f_c}} \cdot \sqrt{\left(1 + \frac{4}{\alpha^2}\right)} \quad (13)$$

$$\tau = \gamma \cdot \sqrt{f_c} \quad (14)$$

The proposed shear strength formulation can be used to predict the actual values of shear stress in the lap splice region. The ultimate shear stress, $\tau_{ult} = \gamma_{ult}\sqrt{f_c}$, is calculated according to Eqs. (12)-(14), where f_c is the increased concrete compressive strength due to the confinement provided by the jacket. The design value of the parameter γ (γ_{cal}), the actual value, γ_{exp}, and the value γ_{avail}, which corresponds to the shear stress developed along the actual length of lap splice, are subsequently computed and compared with γ_{ult}.

Therefore, when the calculated shear stress is lower than the ultimate strength, $\tau_{cal} = \gamma_{cal}\sqrt{f_c} < \tau_{ult}$, then the predicted actual value of the lap splice shear stress will be near τ_{cal}, because the lap splice permits yielding of reinforcement ($\tau_{pred} = \tau_{cal}$).

Otherwise, when the computed shear stress is greater or equal to the ultimate capacity of the lap splice region, $\tau_{cal} \geq \tau_{ult}$, the lap splice fails and slipping of the bars occurs prior to the yielding of reinforcement. Nevertheless, the following should also be taken into account for the predicted actual value of the lap splice shear stress:

1. The confinement has a beneficial effect on bond conditions between the concrete and steel bars, while it also prevents the formation and rapid propagation of splitting cracks in the concrete. Thus, in case of poorly confined lap splices (by transverse reinforcement which is inadequate to allow yielding of reinforcement), the observed strain of the lap-spliced bars would be slightly increased with respect to that of totally unconfined lap-spliced reinforcement. Ultimately, failure results from the exhaustion of ultimate concrete shear capacity and the predicted actual value of the lap splice shear stress will be near τ_{ult} ($\tau_{pred} = \tau_{ult}$).
2. In case of totally unconfined lap splices two distinguished sub-cases exist:
   a. The length of the lap splice, l_s, is minor than that required for the yielding of reinforcement, l_b, ($l_s < l_b$):
   Then the failure results from the exhaustion of ultimate concrete shear capacity and the predicted actual value of the lap splice shear stress will be near τ_{ult} ($\tau_{pred} = \tau_{ult}$).
   b. The length of the lap splice, l_s, is inadequate and extremely short compared to the length, l_b, that allows yielding of the bars ($l_s \ll l_b$):
   In this case the developed shear stress is lower than the ultimate shear strength of the concrete in the lap splice region, while premature bond-slip failure dominates the lap splice behaviour. Excessive slipping of the bars (especially plain bars) occurs due to early loss of the bond between concrete and steel bars prior to the exhaustion of ultimate concrete shear capacity. Thus, the predicted actual value of the lap splice shear stress will be near $\tau_{avail} = \gamma_{avail}\sqrt{f_c} < \tau_{ult}$, ($\tau_{pred} = \tau_{avail}$).

The validity of the proposed formulation was checked using test data for 8 column subassemblages that were tested in the Laboratory of Reinforced Concrete Structures and Masonry Buildings of the Aristotle University of Thessaloniki, as well as data from 23 similar experiments carried out in the United States of America (see Fig. 12).

The shear capacities of the lap splice region of the

Table 3 Predicted-versus-experimental concrete shear stress value in the potential failure plane

	O_1	O_2	SG_1	SG_2	SE_1	SE_2	RHN_1	RHN_2
$\frac{\tau_{pred}}{\tau_{exp}}$	1.17	0.93	1.09	1.11	1.00	1.00	1.00	1.00

Table 4 Experimental and predicted values of concrete shear stress in the potential failure plane

Specimen	f_c (Mpa)	f'_c (Mpa)	γ_{cal} (Mpa)	γ_{ult} (Mpa)	γ_{avail} (Mpa)	γ_{exp} (Mpa)	γ_{pred} (Mpa)	τ_{exp} (Mpa)	τ_{pred} (Mpa)
O_1	−	9.81	1.57	0.506	0.28	0.24	0.28	0.75	0.877
O_2	−	8.80	1.38	0.48	0.29	0.31	0.29	0.920	0.860
SG_1	13.05	8.51	1.36	0.58	−	0.53	0.58	1.915	2.090
SG_2	15.20	10.65	1.05	0.62	−	0.56	0.62	2.183	2.417
SE_1	31.82	9.04	0.87	0.91	−	0.87	0.87	4.910	4.910
SE_2	31.70	8.93	0.73	0.91	−	0.73	0.73	4.110	4.110
RHN_1	60.00	9.63	0.63	1.25	−	0.63	0.63	4.880	4.880
RHN_2	60.00	8.65	0.53	1.25	−	0.53	0.53	4.105	4.105

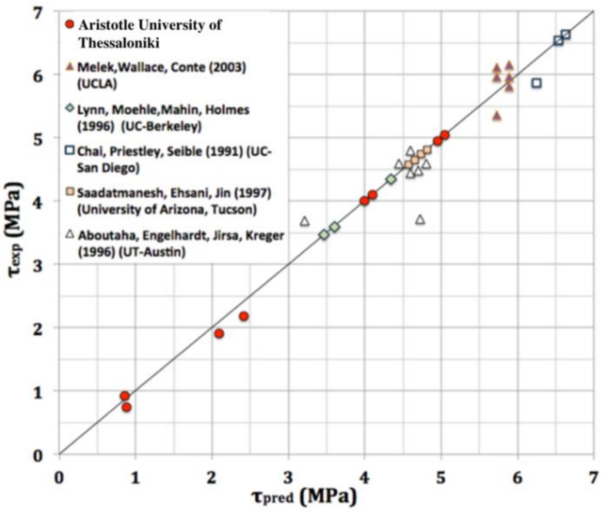

Fig. 12 Experimental-versus-predicted values of shear stress in the lap splice region according to the proposed formulation

original and strengthened specimens were computed using the above methodology (see Table 4). In both cases, the observed capacity was predicted to within approximately 10 percent of that computed using the joint shear strength formulation (see Table 3 and Fig. 12).

8. Conclusions

The following conclusions are drawn based on the work presented herein:

• The original column subassemblages O_1 and O_2, with deficient lap splices of $20d_s$ and $24d_s$ length, exhibited severe degradation of their overall hysteresis behaviour, due to premature bond failure and excessive slipping of the lap-spliced reinforcement. The specimens eventually collapsed under axial loading. This brittle failure may lead to partial or even total collapse of existing pre1960s-70s RC structures.

• The P-Δ effect significantly deteriorates the overall seismic performance of the columns of series I.

• The cyclic response of specimens SG_1 and SG_2, strengthened with steel jackets of 1 mm thickness, was rather poor. Their hysteresis behaviour was governed by the excessive slippage of the bars and the detrimental impact of the P-Δ effect. As a result, rapid degradation of lateral strength, peak-to-peak stiffness and energy dissipation capacity was observed.

• In the case of specimens SE_1 and SE_2, strengthened with steel jackets of 5 mm thickness, yielding of the lap-spliced reinforcement was achieved. Moreover, the seismic behaviour of the enhanced column SE_2, with lap splices of $24d_s$ length, was similar to that of the control subassemblage, C_1, with the continuous longitudinal reinforcement.

• The strengthened specimens of series II showed a ductile seismic behaviour and an indisputable superiority in the overall hysteretic response with respect to the original columns. Moreover, the enhanced subassemblages RHN_1 and RHN_2 showed a cyclic performance similar to that of the control specimen of series II, RC_2. The spindle-shaped hysteresis loops of the specimens clearly demonstrate minor and insignificant impact of the P-Δ effect to the behavior of the columns, while the absence of pinching around the axes indicate that effective restriction of bar slipping was achieved.

• The strengthening scheme applied to the column specimens of series II included the use of additional ties, calculated according to the GCI (Eq. (3)). The latter were particularly used to ensure yielding of the lap-spliced reinforcement. These ties were not part of the transverse reinforcement of the RC jacket. The strengthening process proved to be successful.

• The proposed analytical model successfully predicts the behaviour of lap splices of columns subjected to seismic loading. In the case of unconfined lap splices failure is caused by the early loss of bond stress between steel bars and concrete. In the case of poorly confined lap splices failure is caused by the exhaustion of the concrete ultimate shear capacity in the critical failure plane between the bars. Otherwise, if adequate confinement is provided, yielding of the lap-spliced bars would be achieved.

• The proposed analytical model can be used in both the cases of existing old-type RC structures and the modern ones, while also accurately determining the amount of confinement required to ensure restriction of bar slipping and yielding of the column lap-spliced reinforcement. Thus, reliable design of the retrofit scheme can be achieved.

References

Aboutaha, R.S., Engelhardt, M.D., Jirsa, J.O. and Kreger, E.M. (1996), “Retrofit of concrete columns with inadequate lap splices by the use of rectangular steel jackets”, *Earthq. Spectra*,

12(4), 693-614.

Aboutaha, R.S., Engelhardt, M.D., Jirsa, J.O. and Kreger, M.E. (1999), "Rehabilitation of shear critical concrete columns by use of rectangular steel jackets", *ACI Struct. J.*, **96**(1), 68-78.

Chai, H.Y., Priestley, M.J.N. and Seible, F. (1991), "Seismic retrofit of circular bridge columns for enhanced flexural performance", *ACI Struct. J.*, **88**(5), 572-584.

Chalioris, C., Favatta, M. and Karayannis, C. (2008), "A new method for the seismic rehabilitation of old exterior reinforced concrete beam-column joints", *Proceedings of the 7th European Conference on Struct. Dyn.*, Southampton, UK E245.

Choi, E., Chung, Y.S., Park, K. and Jeon, J.S. (2013), "Effect of steel wrapping jackets on the bond strength of concrete and the lateral performance of circular rc columns", *Eng. Struct.*, **48**, 43-54.

CSRTC (2008), New Code of Steel Reinforcement Technology for Concrete, Athens, Greece.

Daudey, X. and Filiatrault, A. (2000), "Seismic evaluation and retrofit with steel jackets of reinforced concrete bridge piers detailed with lap-splices", *Can. J. Civil Eng.*, **27**(1), 1-16.

Durrani, A.J. and Wight, JK. (1987), "Earthquake resistance of reinforced concrete interior connections including a floor slab", *ACI J. Proc.*, **84**(84-S42), 400-406.

Ehsani, M. (2010), "FRP super laminates", *ACI Concrete Int.*, **32**(3), 49-53.

Ehsani, M.R. and Wight, J.K. (1985), "Effect of transverse and slab on behavior of reinforced concrete beam-to-column connections", *ACI J. Proc.*, **82**(17), 188-195.

Ehsani, M.R. and Wight, J.K. (1985), "Exterior reinforced concrete beam-to-column connections subjected to earthquake - type loading", *ACI J. Proc.*, **82**(4), 492-499.

El Gawady, M., Endeshaw, M., McLean, D. and Sack, R. (2010), "Retrofitting of rectangular columns with deficient lap splices", *J. Compos. Constr.*, **14**(1), 22-35.

EN 1992-1-1 Eurocode 2 (2004), Design of Concrete Structures. Part 1-1: General Rules and Rules for Buildings, 224.

EN 1998-1 Eurocode 8 (2004), Design of Structures for Earthquake Resistance. Part 1: General Rules, Seismic Actions and Rules for Buildings, Stage 51, 229.

Greek Code for Interventions (2017), Earthquake Planning and Protection Organisation, Athens.

Hackman, L., Farell, M. and Dunhan, O. (1992), "Slurry infiltrated mat concrete (SIMCON)", *Concrete Int.*, **14**(12), 53-56.

Hakuto, S., Park, R. and Tanaka, H. (2000), "Seismic load tests on interior and exterior beam-column joints with substandard reinforcing details", *ACI Struct. J.*, **97**(1), 11-25.

Hamilton, H.C., Pardoen, C.G., Navalpakkam, S. and Kanzanjy, P.R. (2004), "Reinforced concrete bridge column performance enhancement through shotcrete jacketing", *ACI Struct. J.*, **101**(3), 332-340.

Henager, C.H. (1997), "Steel fibrous ductile concrete joints for seismic-resistant structures. Reinforced concrete structures in seismic zones", ACI Special Publications SP-53, American Concrete Institute, Detroit, USA.

Julio, N.B.S.E. and Branco, A.B.F. (2008), "Reinforced concrete jacketing-interface influence on cyclic loading response", *Struct. J.*, **105**(4), 471-477.

Kalogeropoulos, G. and Tsonos, A.D. (2014), "Effectiveness of r/c jacketing of substandard r/c columns with short lap splices", *Struct. Monit. Maint.*, **1**(3), 273-292.

Kalogeropoulos, G., Tsonos, A.D., Konstandinidis, D. and Tsetines, S. (2016), "Pre-earthquake and post-earthquake retrofitting of poorly detailed exterior RC beam-to-column joints", *Eng. Struct.*, **109**, 1-15.

Karayannis, C., Chalioris, C. and Sirkelis, G. (2008), "Local retrofit of exterior beam-column joints using thin RC jackets - an experimental study", *Earthq. Eng. Struct. Dyn.*, **37**, 727-746.

Karayannis, C.G. and Sirkelis, G.M. (2008), "Strengthening and rehabilitation of rc beam-column joints using carbon-FRP jacketing and epoxy resin injection", *Earthq. Eng. Struct. Dyn.*, **37**(5), 769-790.

Lynn, A.C., Moehle, J.P., Mahin, S.A. and Holmes, W.T. (1996), "Seismic evaluation of existing reinforced concrete building columns", *Earthq. Spectra*, **12**(4), 715-739.

Melek, M. and Wallace, J.W. (2004), "Cyclic behavior of columns with short lap splices", *ACI Struct. J.*, **101**(6), 802-811.

Pampanin, S., Bolognini, D. and Pavese, A. (2007), "Performance-based seismic retrofit strategy for existing reinforced concrete frame systems using fiber-reinforced polymer composites", *J. Compos. Constr.*, **11**(2), 211-226.

Paulay, T. (1982), "Lapped splices in earthquake-resisting columns", *ACI Struct. J.*, **79**(6), 458-469.

Paulay, T. and Priestley, M.J.N. (1992), *Seismic Design of Reinforced Concrete and Masonry Vuildings*, John Wiley and Sons, New York, NY, USA.

Pavese, A., Bolognini, D. and Peloso, S. (2004), "FRP seismic retrofit of RC square hollow section bridge piers", *J. Earthq. Eng.*, **8**(1), 225-250.

Rodriguez, M. and Park, R. (1994), "Seismic load tests on reinforced concrete columns strengthened by jacketing", *ACI Struct. J.*, **91**(2), 150-159.

Saadatmanesh, H., Ehsani, M.R. and Jin, L. (1997), "Repair of earthquake-damaged RC columns with FRP wraps", *ACI Struct. J.*, **94**(2), 206-214.

Tsonos, A. (2007b), "Steel fiber reinforced concrete of high-strength for the construction of jackets for earthquake-strengthening of buildings without the use of conventional reinforcement", Patent No 1005657 awarded by the Greek Industrial Property Organization (OBI).

Tsonos, A.D. (2010), "Performance enhancement of R/C building columns and beam-column joints through shotcrete jacketing", *Eng. Struct.*, **32**(3), 726-740.

Tsonos, A.D. (2014), "An innovative solution for strengthening of old R/C structures and for improving the FRP strengthening method", *Struct. Monit. Maint.*, **1**(3), 323-338.

Tsonos, A.D. (2019), "Model for the evaluation of the beam-column joint ultimate strength-a more simplified version", *Earthq. Struct.*, **16**(2), 141-148.

Tsonos, A.D., Kalogeropoulos, G., Iakovidis, P. and Konstantinidis, D. (2017), "Seismic retrofitting of pre-1970 RC bridge columns using innovative jackets", *Int. J. Struct. Eng.*, **8**(2), 133-147.

Tsonos, A.G. (2007a), "Cyclic load behaviour of reinforced concrete beam-column subassemblages of modern structures", *ACI Struct. J.*, **194**(4), 468-478.

Tsonos, A.G. (2008), "Effectiveness of CFRP-jackets and r/c-jackets in post-earthquake and pre-earthquake retrofitting of beam-column subassemblages", *Eng. Struct.*, **30**(3), 777-793.

Yeh, Y. and Mo, Y. (2005), "Shear retrofit of hollow bridge piers with carbon fiber-reinforced polymer sheets", *J. Compos. Constr.*, **9**(4), 327-336.

AT